66-440

AN ACOUSTIC WIND MEASURING TECHNIQUE

by

WESLEY W. BUSHMAN
University of Michigan
Ann Arbor, Michigan
and
ORVEL E. SMITH
National Aeronautics and Space Administration
Huntsville, Alabama

AIAA Paper
No. 66-440

AIAA
4th Aerospace Sciences Meeting
LOS ANGELES, CALIFORNIA / JUNE 27-29, 1966

AN ACOUSTIC WIND MEASURING TECHNIQUE

Wesley W. Bushman
Space Physics Research Laboratory
University of Michigan, Ann Arbor, Michigan
Orvel E. Smith
Aero-Astrodynamics Laboratory
Marshall Space Flight Center, Huntsville, Alabama

ABSTRACT

An atmospheric wind measurement technique has been developed and used to measure wind profiles over Cape Kennedy from ground to 85 kilometers. The technique is an extension of the Rocket Grenade Experiment utilizing as its sound source, rather than a grenade, the acoustic noise of a rocket's exhaust. To determine the wind profile from this continuous sound source, a set of equations has been derived and applied to measurements made during the flights of several Saturn vehicles. The profiles agree well with concurrent measurements at lower altitudes (below 50 km.) and are consistent with atmospheric circulation observations at higher altitudes. A preliminary error analysis indicates that the technique can be used to make measurements of sufficient precision to be useful in engineering and meteorological studies.

The research reported here is supported by the NASA George C. Marshall Space Flight Center through Contracts NAS8-11054 and NAS8-20357.

I. Introduction

The problem of measuring winds in the upper stratosphere and above has received considerable attention since sounding rockets have rendered these altitude regions accessible to direct measurements. Interest in the winds comes primarily from two sources. First, since atmospheric motions are related to thermodynamic quantities such as temperature, pressure and density and since they play a role in energy exchange processes, knowledge of these motions is essential to scientific understanding of the atmosphere. Second, atmospheric wind research has gained technological importance because of requirements of aerospace vehicle research and development programs.

The importance of atmospheric wind research is evident from the many efforts directed toward wind measurement. Among the experiments currently being used are: Free lift balloons, such as the double and triple theodolite techniques, Jimsphere[1] and rawinsonde; meterological rocket deployed sensors; Robin balloon chaff and parachute; the Rocket Grenade[2,3] and Sodium Vapor[4] experiments. Each of these experiments has recognized altitude range limitations; i.e., to measure the wind profile from ground to 85 km. two or three separate systems are used.

The Rocket Exhaust Noise Technique presented here offers the capability of economically deriving wind profiles from ground to 85 km. altitude. The technique is similiar to the Grenade

Experiment to the extent that both are based on the atmospheric temperature and mass motion dependence of the velocity of sound. In the Grenade Experiment average temperatures and winds between adjacent grenade detonations are determined by measuring the time required for sound to travel from a source of known position to a ground based microphone array, and its angle of arrival at the array.

When rocket exhaust noise is used as a sound source, the times and locations of the many noise events that characterize the exhaust are not known. If, however, the temperature is measured independently, then the arrival angles of the noise events can be used to determine winds. A ground based array of microphones intercepts the acoustic wave front of the noise and the time of arrival at individual microphones is used to calculate arrival angles. The noise event is traced back by an iterative process until it correctly intersects the vehicle trajectory. Each noise event so traced leads to a wind data point, giving rise to a wind profile in a stratified atmosphere with the average wind in each layer between selected noise events.

The assumptions made for the approach described here are:

(1) The vertical component of wind is negligible compared with the local speed of sound.

(2) The source of sound is considered to be a point located at the nozzle of the engine or a known distance behind

along the flight path. The sound wave is approximated by a plane wave at large distances from the source.

(3) The atmosphere remains in a steady state for the duration of the measurement, i.e., no changes with respect to time in the wind velocities and temperature.

II. The Experiment

2.1 The Measurement

A cross shaped array of nine microphones was set up on the southeast point of Cape Kennedy to monitor launchings of space vehicles. A minimum of three microphones is necessary to determine the arrival angle of the sound, the additional microphones provide redundancy and increased accuracy.

The size of the microphone array shown in Fig. 1 is about 1200 meters along each axis. This size was chosen to maximize the accuracy of the experiment with respect to two sources of error:

(1) Errors which decrease with increasing array size introduced from finite resolution in reading arrival times and

(2) Errors which increase with array size introduced by the plane wave assumption.

The microphones are hot wire, single chamber Helmholtz resonators tuned to about 4 cycles/sec. This low frequency is particularly well suited to extremely far field acoustic measurements since the atmosphere tends to be a low pass filter over long

distances. The microphones were designed at Texas Western College for use in the Rocket Grenade Experiment.

The microphones are situated in heavily vegetated locations to minimize local wind noise. Each microphone is contained in a concrete box, recessed so its top is level with the ground surface. These boxes also serve as permanent survey markers defining the geodetic position of each microphone to within 6 inches.

The electronic and recording equipment is housed in a van located near microphone 4. Although a location near microphone 1 would require about 2 1/2 miles less cable, it was considered desirable to keep the van removed from the array to reduce the possibility of reflective interference.

For the Saturn series of launches the exhaust noise was audible to the microphones from launch until the vehicle was about 100 km. slant distance. Because of the wide range of sound levels, a manually operated variable attenuator was used to maintain the proper signal level into a magnetic tape recorder. Range time is simultaneously recorded with the microphone outputs.

2.2 Theory

The theory and data reduction can conveniently be treated in three steps.

1) Cross correlation to determine arrival times.

2) Ray tracing through layers of known temperature and wind.

3) Solution for winds in the unknown layer.

2.2.1 Cross correlation to determine arrival times.

In the absence of local interference, the acoustic wave front of a noise event appears essentially identical to microphones at separated locations. If identical microphones are used, the output wave form of one microphone matches that of another - shifted in time. The first step in the data analysis is the cross correlation of the microphone output waveforms to determine this time difference. Fig. 2 is a typical record made about 55 seconds after launch of Saturn SA-9. The time differences can be read directly from this type of record.

The manual cross correlation from records such as Fig. 2 is both tedious and subject to human errors. To avoid these problems and to permit rapid reduction of the data, the cross correlation is done automatically on a digital computer. The data from all microphones are digitized and a cross correlation function is computed for each microphone paired with microphone No. 1. This function is defined as

$$R(t') = N \int_{\substack{\text{SLICE} \\ \text{TIME}}} \psi^{1}(t)\ \psi^{2}(t+t')\ dt$$

where: R is the magnitude of the cross correlation function

t' is the time difference

N is a normalization factor

$\psi^1(t)$ & $\psi^2(t)$ are two time dependent microphone outputs

SLICE TIME is a pre-set integration time interval

A typical plot of R(t') is shown in Fig. 3. The magnitude of R at the principal maximum gives an indication of the degree of match of the waveforms, unity meaning they are identical. The time of occurance of the peak is the time difference between microphones.

2.2.2 Ray Tracing Through Layers of Known Temperature and Wind.

The time difference determined by the cross correlation is a function of the sound arrival angle, speed of sound at the array and microphone placement. The arrival angles (or equivalently the characteristic velocities, K_x and K_y defined as the velocities of intersection of the wave front with the x and y axis) are computed from the time difference with appropriate corrections for microphones not lying precisely on the x or y axis. Since there are five microphones along each axis, four independent measurements of K_x and K_y can be made. This redundancy is used to reduce random errors and to correct for deviations of the wave front from plane.

Milne[5] has shown that the wave normal of the ray reaching the microphones remains parallel to the same vertical

plane throughout its propagation. For a plane wave then, the characteristic velocities of a specific sound ray are constant. Since the temperature and wind are treated as constant in any layer, the segment of the sound ray in that layer is a straight line. The wave front is refracted at each layer interface in a way analogous to the refraction of light waves. This refraction is due to a change in the speed of sound between layers. Further refraction occurs if wind direction and magnitude are not identical across layer boundaries. These considerations lead to an expression similar to Snell's law:

$$W + V \sec \theta = \text{constant} \qquad (1)$$

where: θ is the elevation angle of the wave front normal

V is the local speed of sound

W is the horizontal wind component in the vertical plane containing the wave front normal. The component of wind perpendicular to W simply displaces the ray along the plane of the wave front.

The constant in (1) is determined from the characteristic velocities. It is numerically equal to the characteristic velocity that would be measured along a horizontal axis parallel to W. If the measurements are made along any other two orthogonal axis x and y

$$\frac{1}{(\text{constant})^2} = \frac{1}{K_x^2} + \frac{1}{K_y^2} \qquad (2)$$

These equations can be used to ray trace through layers in which the temperature speed of sound and winds are known. Otterman[3] has simplified the ray tracing calculation by expressing (1) and (2) in terms of quantities easily defined in cartesian coordinates.

Fig. 4 shows the ray tracing of a typical noise event. Since the winds have been computed from the previous noise events, the ray tracing through layers defined by these events proceeds according to equations (1) and (2). The coordinates and time of penetration of the ray at the top of the last layer are found by integrating the effect of the previous layers. Above this point, conventional ray tracing procedures must be abandoned since the wind is unknown. However, two independent requirements are available.

1) The sound ray must intersect the trajectory.
2) The correct intersection point must satisfy the criterion that the time of arrival of the noise event measured from launch equals the time of flight to the intersection plus the time required for the sound to travel from the intersection to the array.

These two conditions uniquely determine the coordinates of the source along the trajectory and the average wind in the interval.

2.2.3 Solution for Winds in the Unknown Layer

Fig. 5 shows the arrival of the j^{th} noise event

at the top of the $(j-1)^{st}$ layer. Since the temperature and wind is assumed constant in this region, the apparent source is the center of a sphere moving with the wind. The direction cosines of the ray can be written by inspection and are

$$\alpha = \frac{x_j + W_x \Delta t_j - \sum_{k=1}^{j-1} \Delta x_k}{V_{avgj} \Delta t_j} \quad \beta = \frac{y_j + W_y \Delta t_j - \sum_{k=1}^{j-1} \Delta y_k}{V_{avgj} \Delta t_j} \quad \gamma = \frac{z_j - z_{j-1}}{V_{avgj} \Delta t_j}$$

$$\text{where } \Delta t_j = \tau_j - T_j - \sum_{k=1}^{j-1} \Delta t_k$$

The characteristic velocities are

$$K_x = -\frac{V_{avgj}}{\alpha} + W_x + W_y \beta/\alpha \qquad K_y = -\frac{V_{avgj}}{\beta} + W_y + W_x \alpha/\beta$$

Simplifying the writing by substituting

$$V = V_{avgj}, \quad x_o = \sum_{k=1}^{j-1} \Delta x_k \text{ etc.}$$

and remembering the trajectory relates x_j y_j and z_j to T_j

The above equations can be rearranged to give

$$F(K_x, K_y, W_x, W_y, T_j, t_o, x_o, y_o, V) =$$

$$(K_x - W_x)(x_j - W_x \Delta t_j - x_o) + V^2 \Delta t_j - W_y (y_j + W_y \Delta t_j - y_o) = 0 \qquad (3)$$

$$G(K_x, K_y, W_x, W_y, T_j, t_o, x_o, y_o, V) =$$

$$(K_y - W_y)(y_j - W_y \Delta t_j - y_o) + V^2 \Delta t_j - W_x (x_j + W_x \Delta t_j - x_o) = 0 \qquad (4)$$

$$H(K_x, K_y, W_x, W_y, T_j, t_o, x_o, y_o, V) =$$

$$(x_j + W_x \Delta t_j - x_0)^2 + (y_j + W_y \Delta t_j - y_o)^2 + (z_j - z_o)^2 - V^2 \Delta t_j^2 = 0 \qquad (5)$$

The above relations F,G,H = 0 are three equations in the three unknowns W_x W_y and T_j. The functional dependence indicated in F,G, and H, although not shown explicitly in the equations, is to be inferred from the previous relations. These equations show only the principle of solution and not the method of computation. A flow chart displaying the computerized solution after time differences are determined is shown in Figs. 6 and 7.

III. Results

Wind profiles have been determined using the Exhaust Noise technique for the launchings of Saturns SA-8, SA-9, SA-10, Ranger 8 and Apollo Saturn AS-201. These wind profiles are presented in Figs. 8 to 12. Also shown, in each case, are winds determined independently by other systems on the same days. The agreement between the data is consistant with the results of the error analysis of the Rocket Exhaust Noise Technique and errors inherent to the other systems used for comparison.

In the cases of Saturns SA-8, SA-9, and SA-10, winds were measured up to first stage burnout which occured at approximately 85 km. The sound level at the ground from the second stage was not sufficiently intense to be useful for wind data.

In the case of Ranger 8, the trajectory was such that the vehicle was 100 km. distant when it was only 45 km. high. Thus, the sound faded into the background noise level before very high altitudes were attained.

The AS-201 first stage burnout occurred at about 60 km. and the second stage did not generate sufficient sound to allow meaningful interpretation of data.

IV. Error Analysis

Four error sources have been considered.

1. Error in the measurement of sound arrival times. This results in errors in the derived values of characteristic velocities.
2. Errors in the speed of sound profile. These can be introduced from inaccurate temperature data or by the finite amplitude effect.
3. Uncertainty in the position of the noise source with respect to the vehicle.
4. Errors introduced from the plane wave assumption.

Investigation of these possibilities has shown that the error in measurement of arrival times is the most significant contributor to wind error by almost an order of magnitude[6], therefore, analysis of the other sources will be omitted from this section.

Equations 3, 4, and 5 can be used to determine the magnitude of the expected errors. The Jacobian of this system of equations is

$$J = \frac{\partial(F,G,H)}{\partial(W_x,W_y,T)} = \begin{vmatrix} F_{W_x} & F_{W_y} & F_T \\ G_{W_x} & G_{W_y} & G_T \\ H_{W_x} & H_{W_y} & H_T \end{vmatrix} \qquad (6)$$

where $\frac{\partial F}{\partial W_x}$ is denoted by F_{W_x} etc.

Then

$$\frac{\partial W_x}{\partial K_x} = -\frac{\begin{vmatrix} F_{K_x} & F_{W_y} & F_T \\ G_{K_x} & G_{W_y} & G_T \\ H_{K_x} & H_{W_y} & H_T \end{vmatrix}}{J} \qquad \text{etc.} \qquad (7)$$

The wind errors caused by an error in measurement of characteristic velocity (arrival time) is then

$$\Delta W_x = \left(\frac{\partial W_x}{\partial K_x}\right) \Delta K_x + \left(\frac{\partial W_x}{\partial K_y}\right) \Delta K_y + \left(\frac{\partial W_x}{\partial x_o}\right) \Delta x_o + \left(\frac{\partial W_x}{\partial y_o}\right) \Delta y_o + \left(\frac{\partial W_x}{\partial t_o}\right) \Delta t_o$$

with a similar equation for ΔW_y. Typical results of computation of ΔW_x and ΔW_y are shown in Figs. 13 and 14.

Repeated reading of arrival times exhibit a scatter that indicates an uncertainty in the arrival times on the order of 2 or 3 ms. The system parameters were chosen on the basis of uncertainties of about half this value. This larger error is attributed to slight differences in microphone characteristics, differences in local background conditions, and to possible acoustic anomalies of the atmosphere.

To the extent that these effects are random they are reduced by use of the computer program for cross correlation since in this program the time difference between two channels is determined by an integration over a present segment of the data rather than from a single waveform characteristic.

The use of higher frequencies of the noise spectrum offers the possibility of increased precision in determining arrival times. Experimentation with wide band microphones is planned to evaluate this possibility.

V. Conclusion

The agreement between the wind profiles determined by the Rocket Exhaust Noise Technique and other simultaneous measurements is evidence of the validity of the acoustic technique described herein.

On the basis of the error analysis, the maximum errors are estimated to be about ±20 m/s at 85 km. and decreasing to about ±7 m/s at 30 km. These errors are attributed principally to inaccuracies in determining arrival time and should be reducible by the use of improved measurement and data reduction techniques.

At locations where large booster rockets are launched regularly, a rather modest ground station can gather wind data from the ground to, in some cases, 85 km. These data measured concurrent with the space vehicle flight have important engineering value, and the upper atmospheric wind profiles measured on a regular basis would be an important supplement to the data available to meterologists.

REFERENCES

1. Scoggins, James R., "Aerodynamics of Spherical Balloon Wind Sensor," Journal of Geophysical Research, Vol. 69, No. 4, February 1964, pp. 591-598.

2. Stroud, W.G., Nordberg, W., and Walsh, J.R., "Temperatures and Winds between 30 and 80 km.,"Journal of Geophysical Research, Vol.61, No.61,45-56, 1956.

3. Otterman, J., "A Simplified Method for Computing Upper Atmosphere Temperature and Winds in the Rocket-Grenade Experiment," Univ. of Mich. Tech. Report 2387-40-T, Army Contract No. DA-36-039-SC-64657, June 1958.

4. Manring, E., Bedinger, J., and Knaflich, H., Space Research II, ed. H.C. van de Hulst et al. (North-Holland Publ. Co., Amsterdam, 1961) 1107

5. Milne, E.A., "Sound Waves in the Atmosphere," Phil. Mag. 42, pp. 96-114, 1921.

6. Bushman, W.W., Kakli, G.M., Carignan, G.R., "An Acoustic Wind Measuring Technique," Univ. of Mich Tech. Report 05911-2-T, Contract NAS8-11054, July 1965.

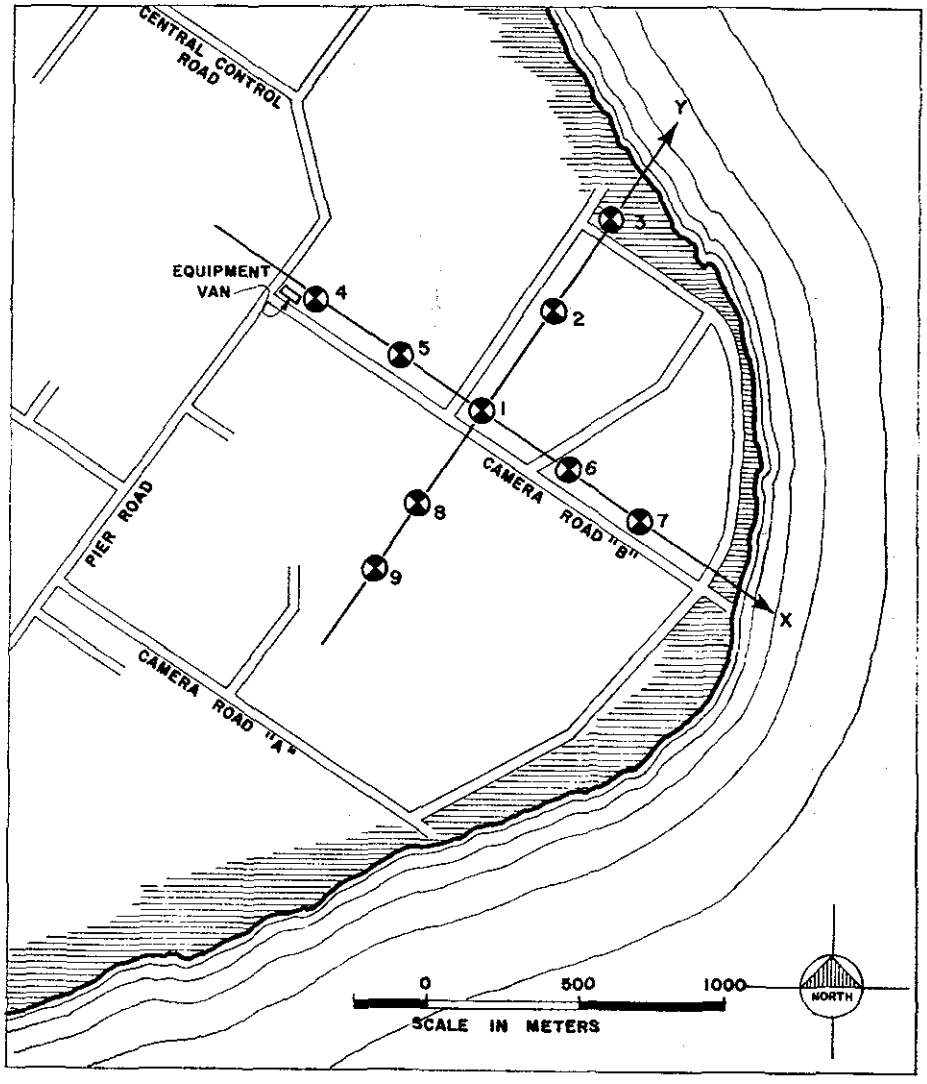

FIG. 1: THE MICROPHONE ARRAY AND COORDINATE SYSTEM

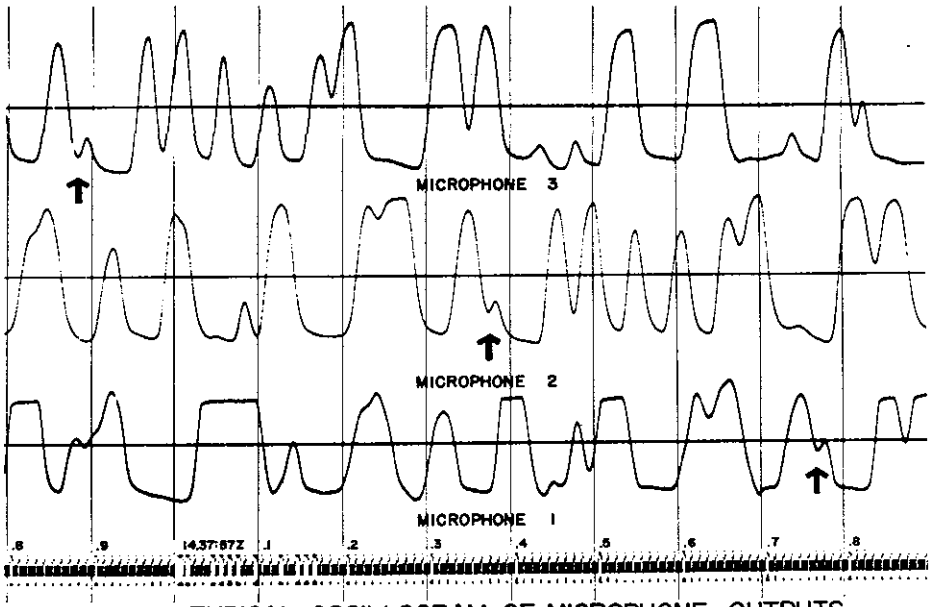

FIG. 2 TYPICAL OSCILLOGRAM OF MICROPHONE OUTPUTS

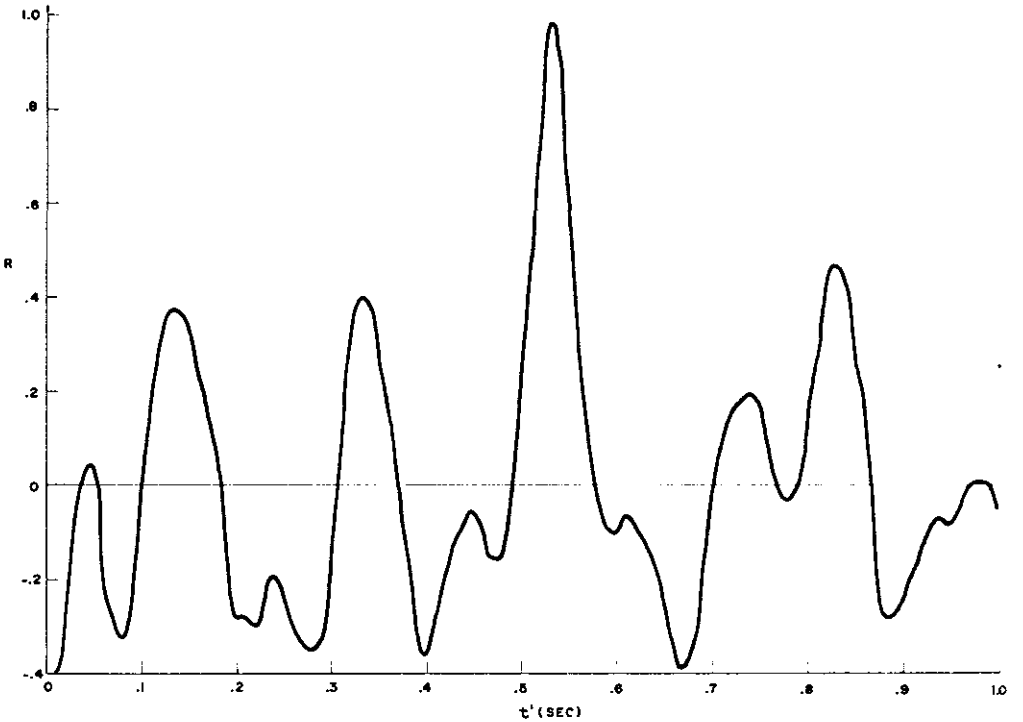

FIG. 3 TYPICAL VARIATION OF CROSS CORRELATION WITH TIME DIFFERENCE

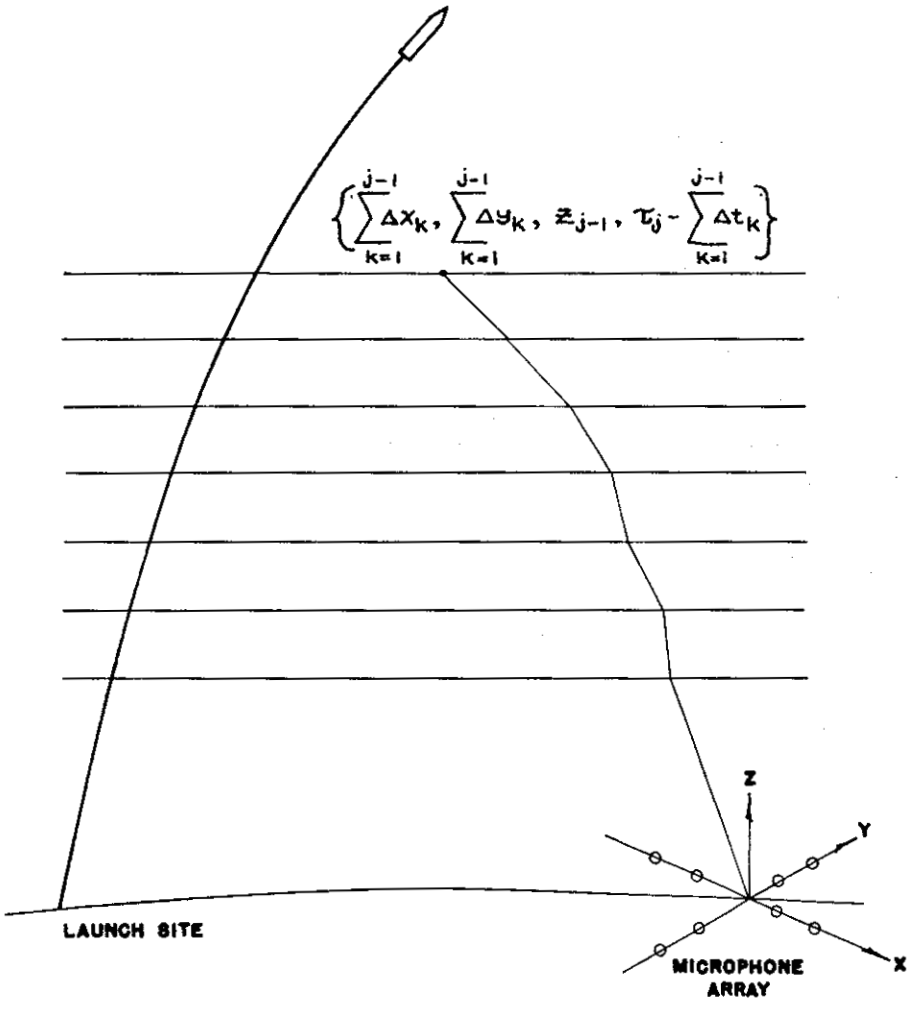

FIG. 4 GEOMETRY OF THE WIND EXPERIMENT

THE SOUND IS HEARD AT THE ARRAY AT TIME τ_j

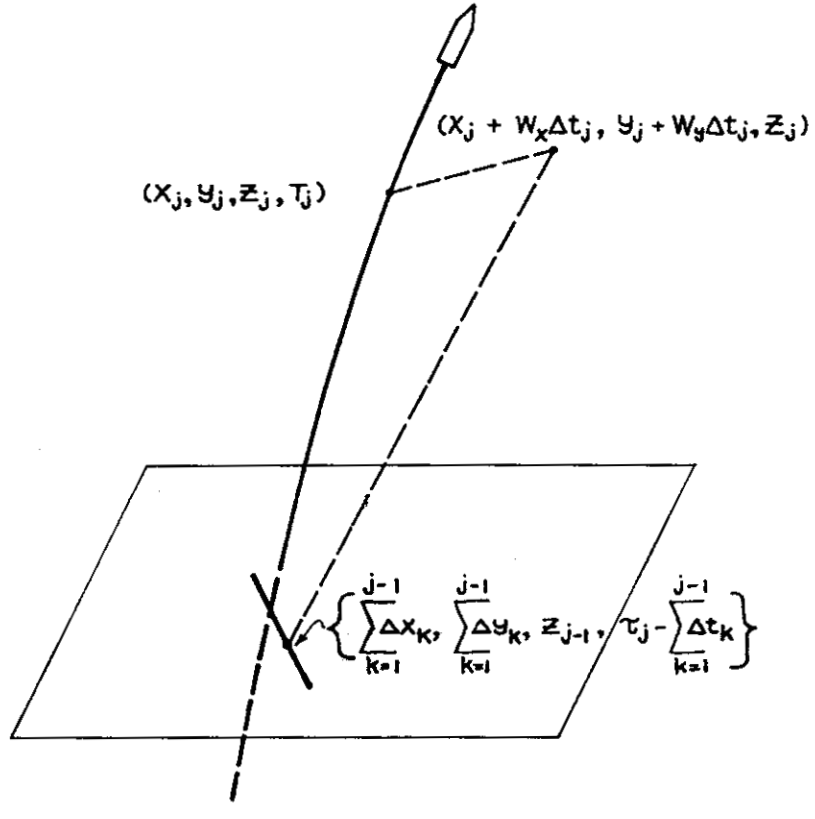

FIG. 5 THE ARRIVAL OF A NOISE EVENT AT THE TOP OF THE LAST KNOWN LAYER.

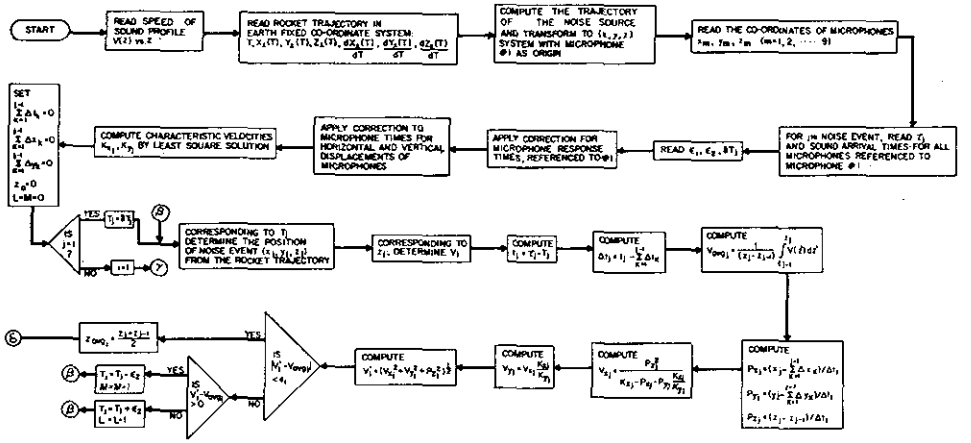

FIG. 6 FLOW DIAGRAM FOR WIND COMPUTATION

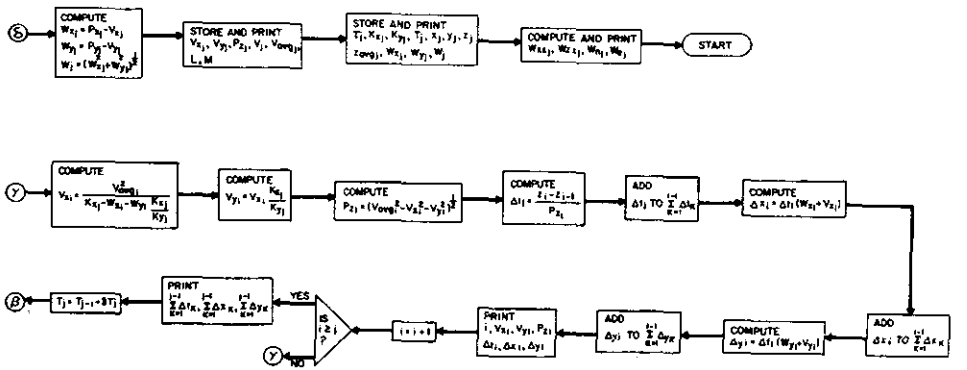

FIG. 7 FLOW DIAGRAM FOR WIND COMPUTATION

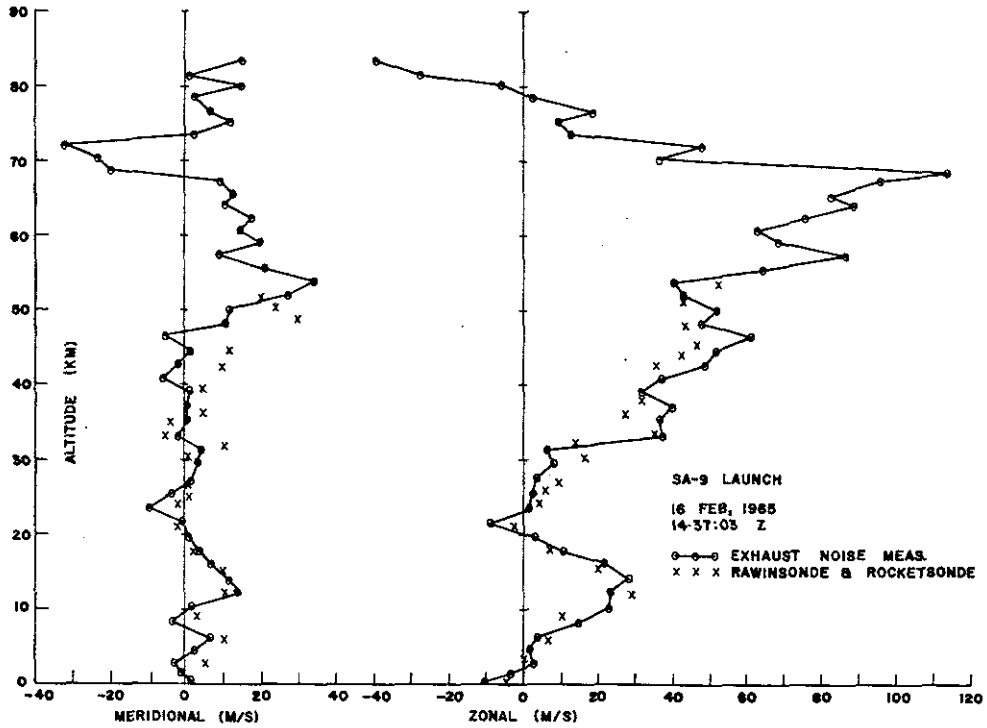

FIG. 8 SA-9 WIND PROFILE

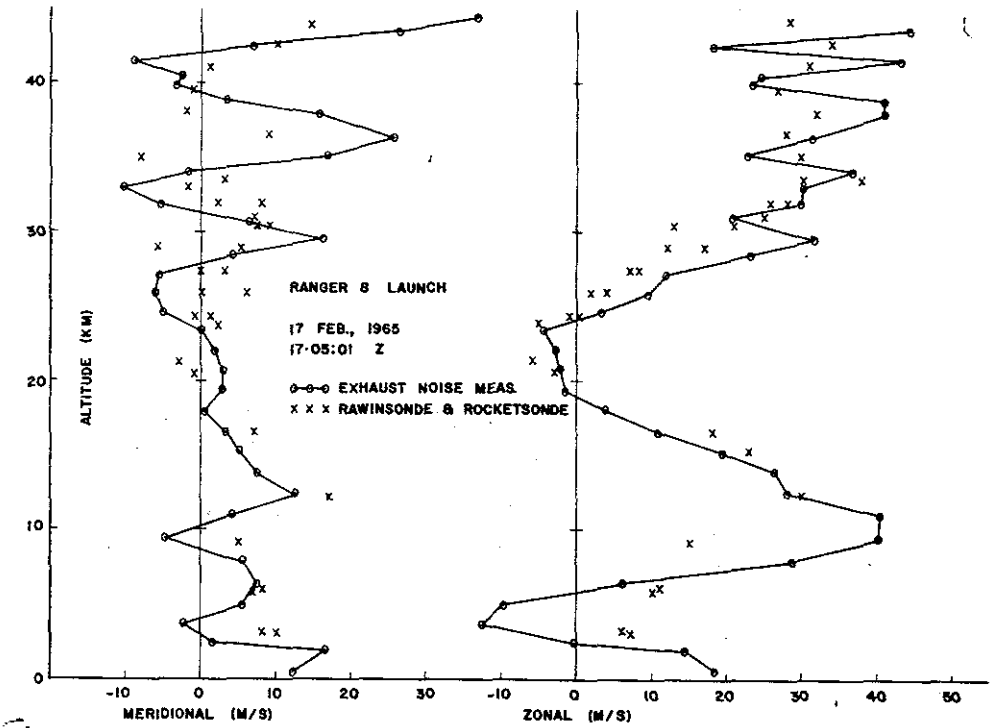

FIG. 9 RANGER 8 WIND PROFILE

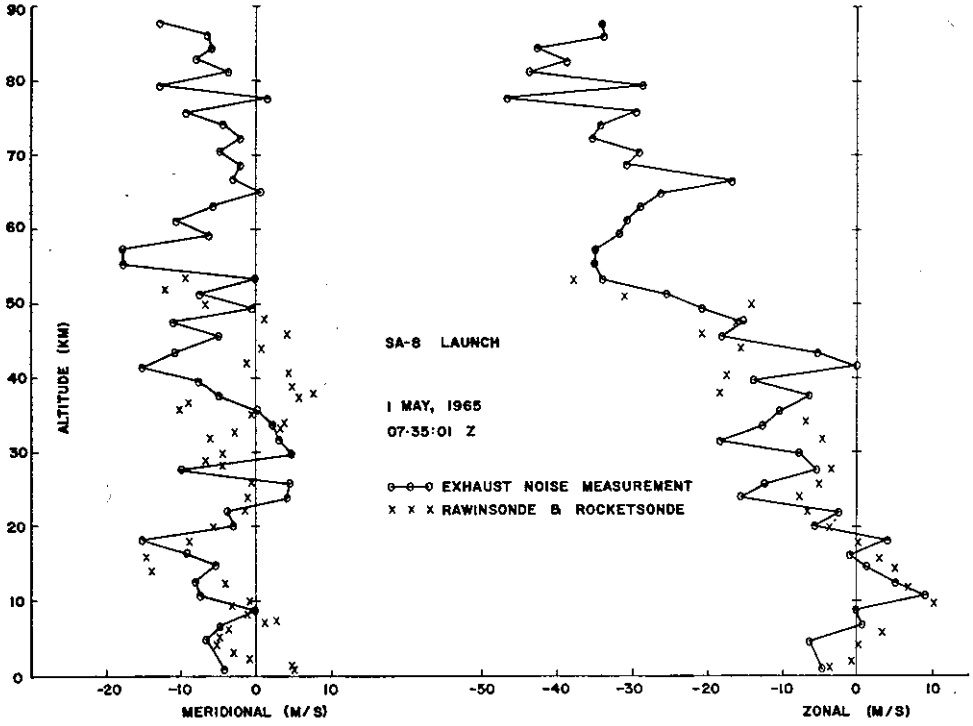

FIG. 10 SA-8 WIND PROFILE

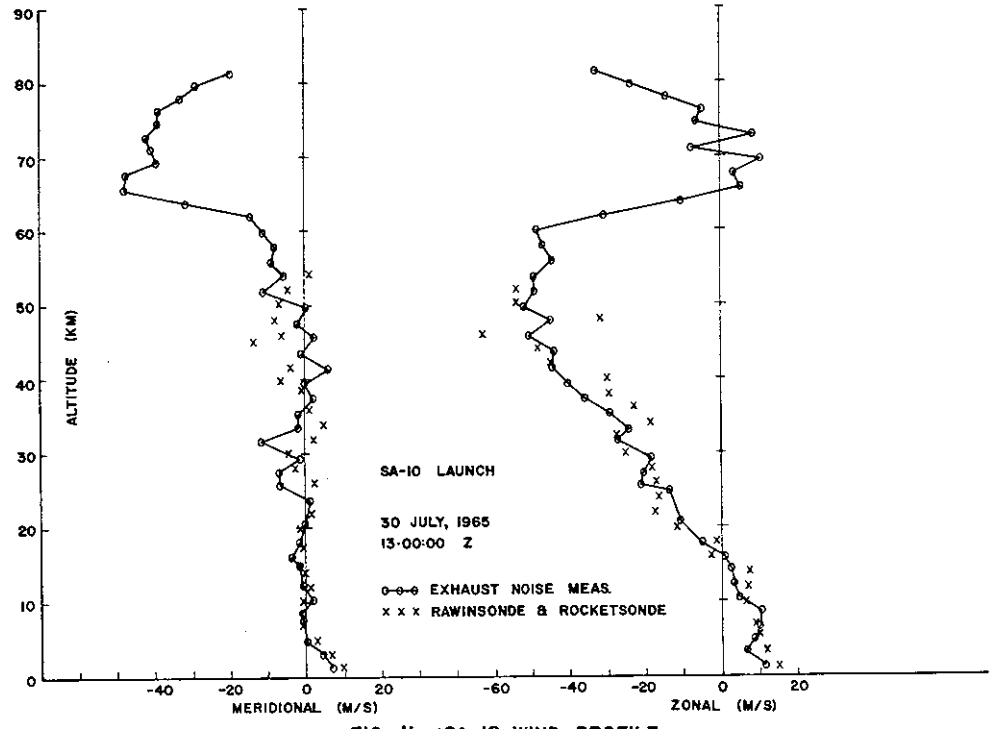

FIG. 11 SA-10 WIND PROFILE

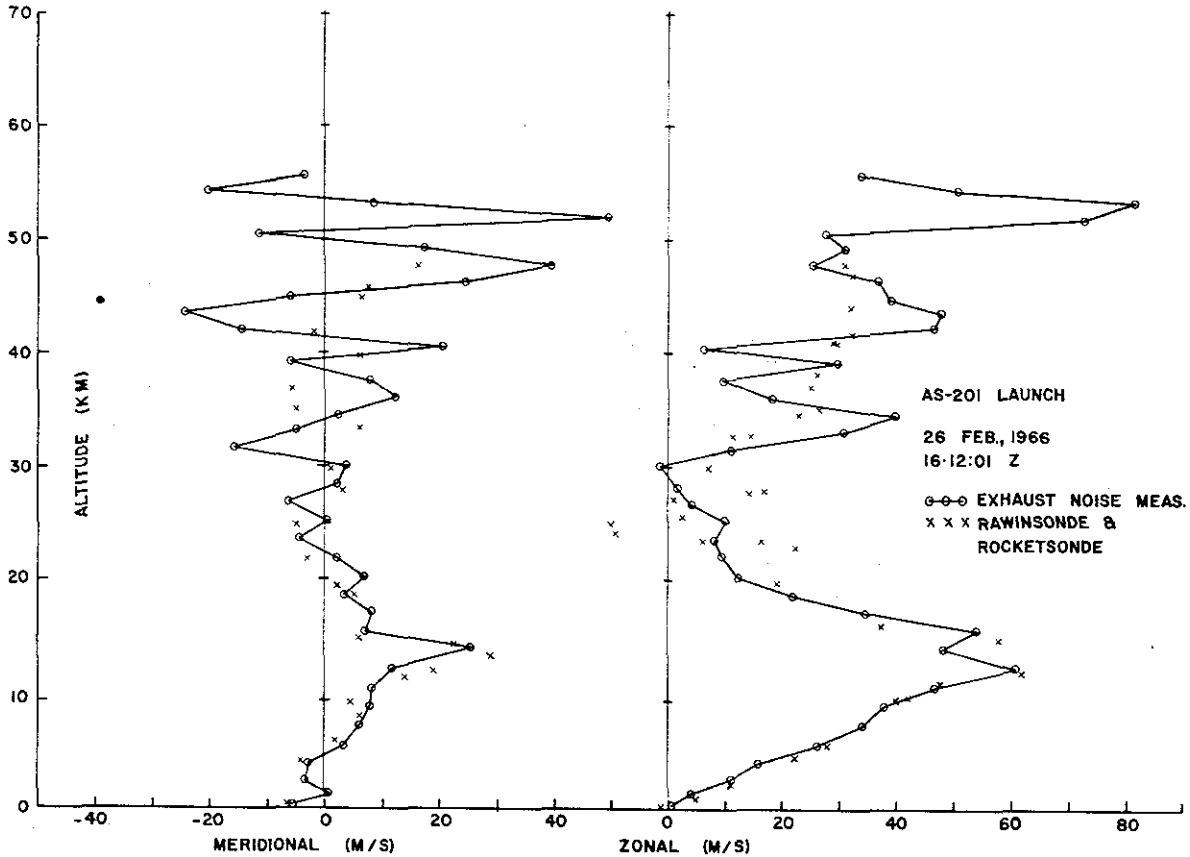

FIG. 12 AS-201 WIND PROFILE

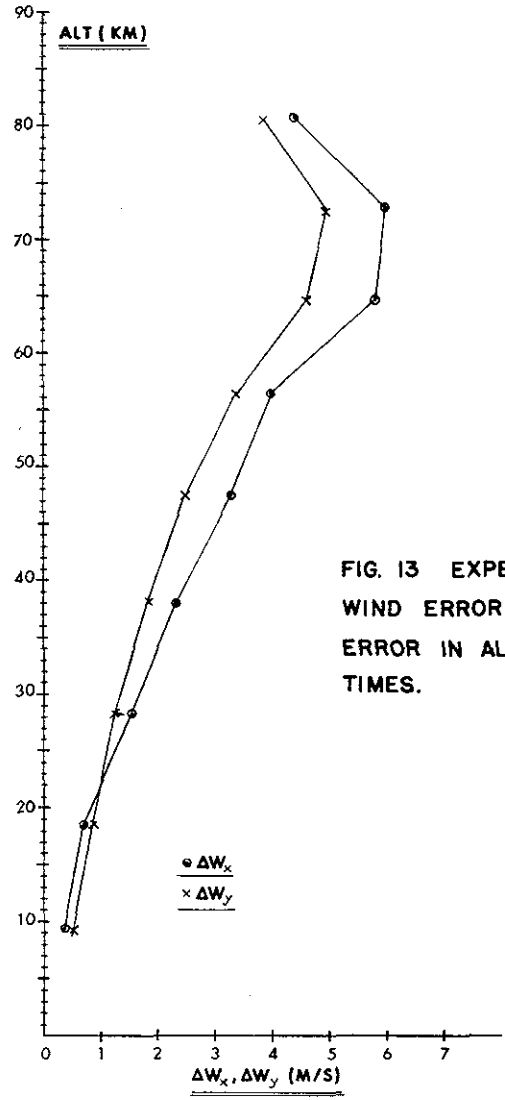

FIG. 13 EXPECTED MAXIMUM WIND ERROR DUE TO .5 MS ERROR IN ALL MICROPHONE TIMES.

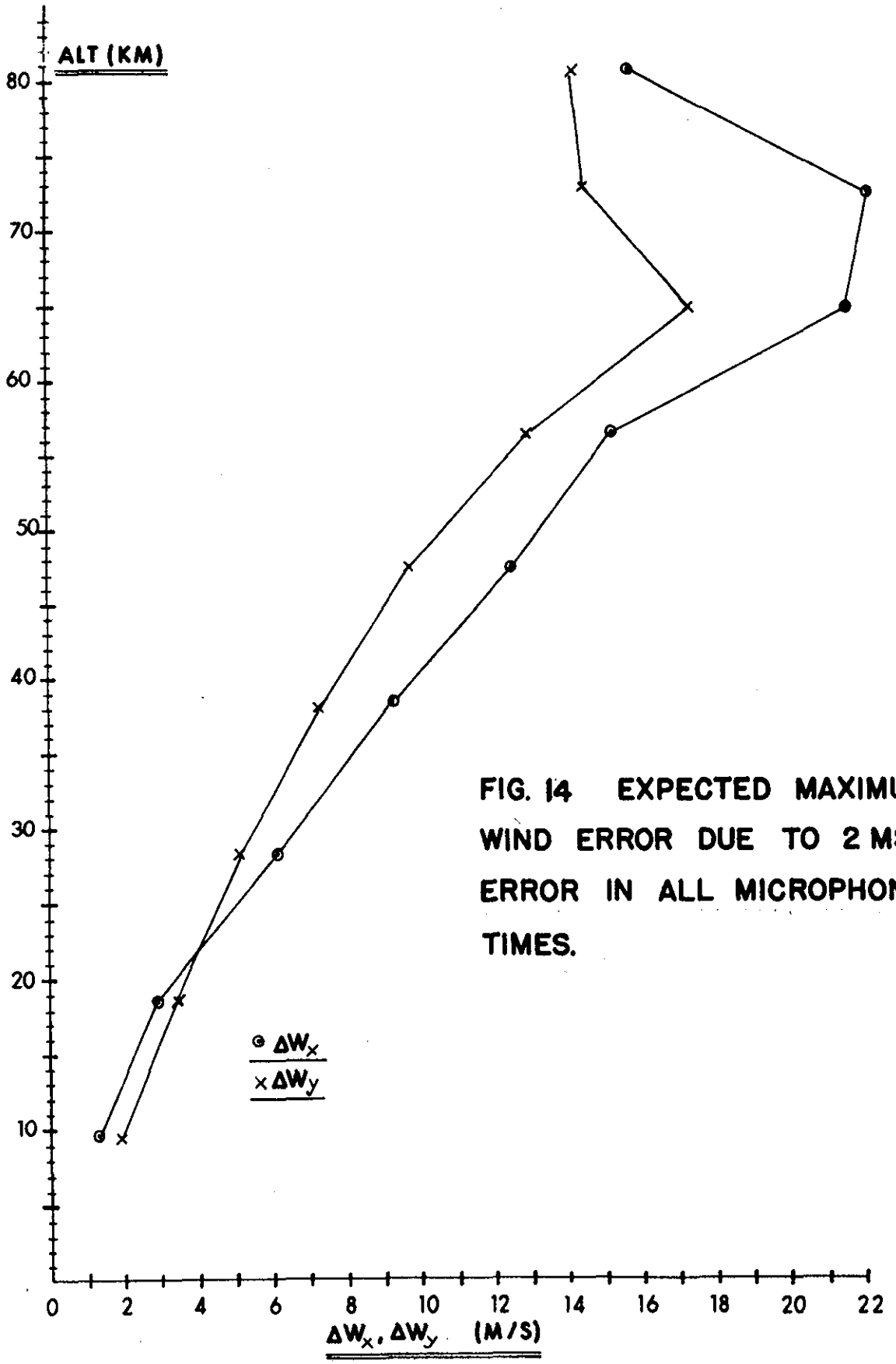

FIG. 14 EXPECTED MAXIMUM WIND ERROR DUE TO 2 MS ERROR IN ALL MICROPHONE TIMES.